

Contents List available at JACS Directory

Journal of Advanced Electrochemistry

journal homepage: http://www.jacsdirectory.com/jaec



Inhibition of Oxadiazole Derivatives for the Control of Corrosion of Copper-Nickel Alloy in Sea Water

K. Chadrasekaran¹, B.S. Alwar², R. Ravichandran^{1,*}

Post Graduate and Research Department of Chemistry, Dr. Ambedkar Government Arts College (Autonomous), Chennai – 600 039, Tamil Nadu, India.

ARTICLE DETAILS

Article history: Received 22 September 2016 Accepted 01 October 2016 Available online 07 October 2016

Keywords: Copper-Nickel Alloy Oxadiazoles Sea Water Impedance Arrhenius Plot

ABSTRACT

Inhibitive action of four oxadiazole derivatives namely 2,5-diphenyl-1,3,4-oxadiazole (DPOX), 2-Amino-5-(4-methoxyphenyl)-1,3,4-oxadiazole(AMOX),2,5-Bis(4-diethylaminophenyl)-1,3,4-oxadiazole(BPOX) and 2,5-Bis-(4-aminophenyl)-1,3,4-oxadiazole (BAOX) on the corrosion of copper-nickel alloy in natural sea water has been studied. Weight loss, potentio-dynamic polarisation measurement and electrochemical impedance spectroscopy (EIS) has been employed to analyse their inhibition behavior of oxadiazole derivatives. Polarization measurements showed that the oxadiazole derivative inhibits the corrosion of copper-nickel alloy by blocking the active sites of the metal surface. Changes in the impedance parameters (charge transfer resistance (Rct) and double layer capacitance (Cdl)) are related to adsorption of organic inhibitors on the metal surface, leading to the formation of a protective film. BAOX showed better protection over the other inhibitor used. The dissolution of copper and nickel in the presence and absence of oxadiazoles was analysed by ICP-AES.

1. Introduction

Copper-based alloys have a long history of service in marine environments. In general, they exhibit an attractive combination of properties, e.g., good machinability, good resistance to corrosion and biofouling and superior thermal and electrical conductivities [1, 2]. In view of their good machinability, they are available in a wide range of products [3]. The 90/10 copper-nickel alloy is a material of selection for condensers and heat exchangers, where seawater is used as a coolant and in desalination plants. Copper-Nickel alloy are also used in sea water pipework, offshore fire water systems, sheathing of legs and risers on offshore platforms and boat hulls, Hydraulic lines and Fish cages for aquaculture. They have provided reliable service for several decades whilst offering effective solutions to today's technological challenges. This alloy is resistant to stress corrosion cracking by ammonia and sulphide ions [4] and has good resistance to bio-fouling due to the release of copper ions [5, 6]. This alloy is also resistant to pitting and crevice corrosion in quiet seawater [7]. The corrosion resistance of this alloy is related to the performance of the passive film, which is mainly composed of Cu₂O [8, 9]. The cupric species generally overlies the cuprous species. However, in the sulphide containing seawater, the corrosion rate of Cu-Ni (90/10) alloy is increased as the sulphide ions interfere with the film formation and produce a nonprotective black layer containing cuprous oxide and sulphide ions [10]. The pollution of seawater with sulphide ions at the coastal areas can occur due to industrial waste water discharges into sea and also due to biological and bacteriological processes taking place in seawater. Thus, corrosion of Cu-Ni alloy in seawater polluted with sulphide ions is a serious problem, which has drawn the attention of the researchers in this field.

Organic compounds containing an "azole nucleus" have frequently been employed to inhibit corrosion of copper and brass mostly in acidic or neutral solution [11]. Among these, benzotriazole (BTA), a sub category of N-heterocyclic compounds is known as one of the best corrosion inhibitors for copper and its alloys in a wide range of environments [12]. Brusic et al. [13] showed that a polymerized network formed and gave significant protection in many environments; the enhanced protection was retained even when the copper was removed from the BTA solution. Badawy et al.

[14] studied the corrosion inhibition of Cu-5Ni and Cu-65Ni alloys in 0.6 moldm $^{-3}$ chloride solution using amino acids as inhibitors. Benmessaoud et al. [15] studied the inhibiting effect of 2-mercaptobenzimidazole against the corrosion of 70Cu-30Ni alloy in aerated 3% sodium chloride solution polluted with ammonia (pH = 9.25) by potentiodynamic polarization studies and electrochemical impedance studies. 1,2,3-benzotriazole is a well-known corrosion inhibitor for copper. Allam et al. [16] studied the effect of benzotriazole on the corrosion of Cu-Ni (90/10) alloy in 3.4% sodium chloride solution containing 2 ppm of sulphide ions by weight-loss measurements and X-ray diffraction technique.

2. Experimental Methods

2.1 Materials

The material used for this study was copper-nickel alloy supplied in the form of sheet and the chemical composition (weight percent) of the alloy is given in Table 1. The natural sea water was collected near National Thermal Power Corporation (NTPC), Ennore, Chennai, India and the chemical composition of the seawater was given in Table 2. The pH of the seawater is 6.5. The inhibitors oxadiazole derivatives (Sigma-Aldrich) and absolute ethanol (Merck) were used as received. The structures of oxadiazole derivatives are shown in Fig. 1.

Table 1 Chemical composition of Cu/Ni (90/10) (in wt%)

Alloy	Cu	Ni	Fe	Mn	Pb	Al	Other trace
							elements
Composition	89.23	9.663	0.682	0.267	0.0594	0.0415	0.0551

Table 2 Composition of polluted natural sea water

Species	Cl-	SO ₄ 2-	S2-	HCO ₃ -	PO ₄ 3-	CO ₃ 2-	NO ₂ -	NO ₃ -	Br-	F-
Concentration	35.24	4.56	2.49	0.94	2.12	1.28	0.24	0.31	0.32	0.04
(g/lit)										

*Corresponding Author

Email Address: varmaravi1965@rediffmail.com (R. Ravichandran)

²Post Graduate and Research Department of Chemistry, D.G. Vaishnav College (Autonomous), Chennai – 600 106, Tamil Nadu, India.

2, 5 - diphenyl-1,3,4-oxadiazole (DPOX)

2 - amino-5-(4-methoxyphenyl)-1,3,4-oxadiazole (AMOX)

2, 5 - bis(4-diethylaminophenyl)-1,3,4-oxadiazole (BPOX)

$$H_2N$$
 $N-N$
 NH_2

2, 5 - bis-(4-aminophenyl)-1,3,4-oxadiazole (BAOX)

Fig. 1 Structures of oxadiazole derivatives

2.2 Methods

For weight-loss method, the copper-nickel alloy specimens (4 cm x 2.5 cm x 0.2 cm) were abraded with silicon carbide papers (120-1200 grit), thoroughly washed with distilled water, degreased with acetone, rinsed with distilled water, dried and weighed. The specimens were immersed in 300 mL of natural sea water, with and without inhibitors at 30 °C for 30 days.

For electrochemical studies, the working electrode with an area of $1\,\mathrm{cm}^2$ was embedded in epoxy resin in a Teflon holder. The electrode was abraded mechanically with silicon carbide papers from 120 to 1200 grit followed by polishing with 5 μm diamond paste. The electrode was thoroughly washed with double distilled water, degreased in acetone for 15 minutes using ultrasonic vibration, rinsed with distilled water and dried. The cell assembly consisted of copper-nickel alloy as working electrode, a platinum foil as counter electrode and a saturated calomel electrode (SCE) as a reference electrode with a Luggin capillary bridge.

Polarization studies were carried out using an electrochemical work station (Model: CHI 760C, CH instruments, USA) at a scan rate of 1 mV/s. The working electrode was immersed in natural sea water (open atmosphere) and allowed to stabilize for 30 minutes [17]. In each case a potential of -1500 mV was then applied for 15 minutes to reduce oxides. The cathodic and anodic polarization curves for copper-nickel alloy specimen in the test solution with and without inhibitors were recorded between -500 to 500 mV at a scan rate of 1 mV/s at a temperature range from 303 K to 343 K. The inhibition efficiencies of the compounds were determined from corrosion current density using the Tafel extrapolation method. A.C. impedance measurements were conducted at room temperature using an AUTOLAB with Frequency Response Analyzer (FRA), which included a Potentiostatic model "Autolab PGSTAT 12. An ac sinusoid of ± 10 mV was applied at the corrosion potential (E_{corr}). The frequency range of 100 kHz to 1 mHz was employed. All potentials are reported vs. SCE.

During the anodic polarization, metal dissolution takes place releasing considerable amounts of metal ions from the material. Hence, the solutions were analyzed to determine the leaching characteristics of the coppernickel alloy. The solution left after polarization measurement was analyzed for copper and nickel by inductively coupled argon plasma-atomic emission spectroscopy (ICP-AES). Solutions containing the optimum concentration of the inhibitor were chosen and a blank was also analyzed for comparision purposes.

3. Results and Discussion

3.1 Weight-Loss Measurements

The weight loss measurements are the best known and simplest of all corrosion monitoring techniques. The corrosion rates and inhibition efficiencies of copper-nickel alloy with different concentrations of DPOX, AMOX, BPOX and BAOX in natural sea water at room temperature (30 °C) are given in Table 3. The corrosion rate (CR) and percentage inhibition efficiency (IE %) were calculated using the following equation [18]

$$\begin{split} \text{CR (mmpy)} &= \frac{87.6 \text{ x W}}{\text{D x A x T}} \\ \text{IE\%} &= \frac{\text{CR}_{\text{(bl)}} - \text{CR}_{\text{(inh)}}}{\text{CR}_{\text{(bl)}}} \text{ x 100} \end{split}$$

where W is the weight-loss, D is the density, T is the immersion time, A is the area of the specimen and CR(inh) and CR are the corrosion rate of copper-nickel alloy in the presence and absence of inhibitors respectively. The corrosion rate decreases with increase in the concentration of the inhibitor. The inhibition efficiency increases with the increase in the concentration of the inhibitor upto the optimum level, thereafter it was found to decrease slightly, which is due to the interaction between adsorbed molecules at the sites. The extent of inhibition depends on the nature and concentration of the inhibitor. The optimum concentration was evaluated on the basis of inhibition efficiency and it was found to be 10-3 M for DPOX, AMOX, BPOX and BAOX in natural sea water. The inhibitors have shown the maximum inhibition efficiency of 87.78, 90.06, 91.11 and 93.08 respectively for DPOX, AMOX, BPOX and BAOX in natural sea water. It can be seen that the values of inhibition efficiency for copper-nickel alloy obtained using substituted oxadiazoles in natural sea water follow the order DPOX > AMOX > BPOX > BAOX.

Table 3 Weight loss measurements of copper-nickel alloy at different concentrations of DPOX, AMOX, BPOX and BAOX in natural sea water

Inhibitor Concentration/ M	Corrosion rate/mmpy	Inhibition Efficiency/ %
DPOX	7.694	-
10-5	4.762	38.11
10-4	3.127	59.35
10-3	0.940	87.78
10-2	0.962	87.50
AMOX		
10-5	4.248	44.79
10-4	2.874	62.64
10-3	0.765	90.06
10-2	0.773	89.95
BPOX		
10-5	3.674	52.25
10-4	2.432	70.99
10-3	0.684	91.11
10-2	0.689	91.04
BAOX		
10-5	3.342	56.56
10-4	2.051	73.34
10-3	0.532	93.08
10-2	0.538	93.01

3.2 Polarisation Studies - Effect of Temperature

The effects of temperature on the rate of dissolution of copper-nickel alloy in natural seawater containing optimum concentration (10^{-3} M) of the investigated inhibitors was tested by polarisation method over a temperature range from 303 to 343 K and are shown in Figs. 2 - 6.

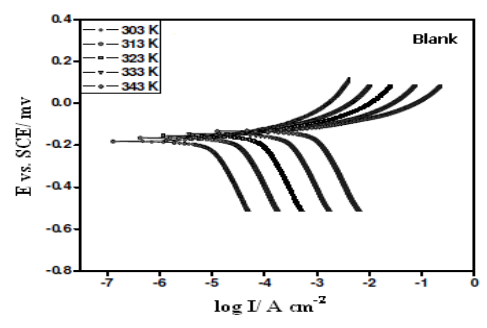


Fig. 2 Tafel plots for copper-nickel alloy in natural sea water without inhibitor at different temperature

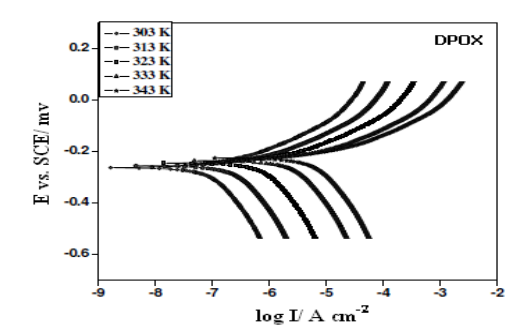


Fig. 3 Tafel plots for copper-nickel alloy in natural sea water in the presence DPOX at different temperature

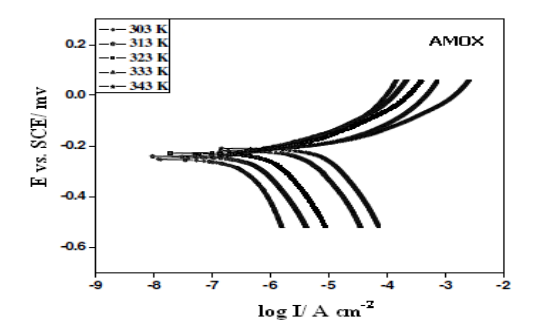
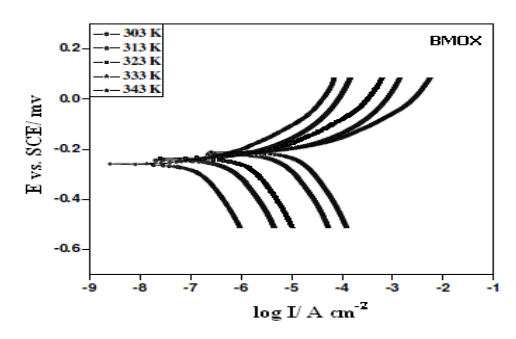
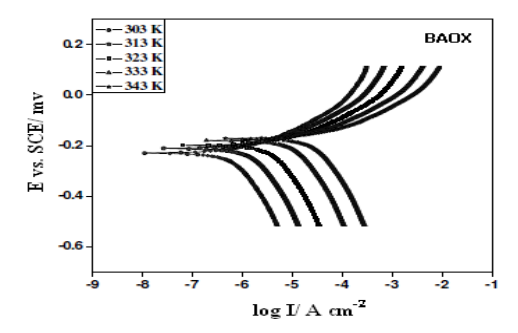


Fig. 4 Tafel plots for copper-nickel alloy in natural sea water in the presence AMOX at different temperature



 $\textbf{Fig. 5} \ \text{Tafel plots for copper-nickel alloy in natural sea water in the presence BMOX} \ \text{at different temperature}$



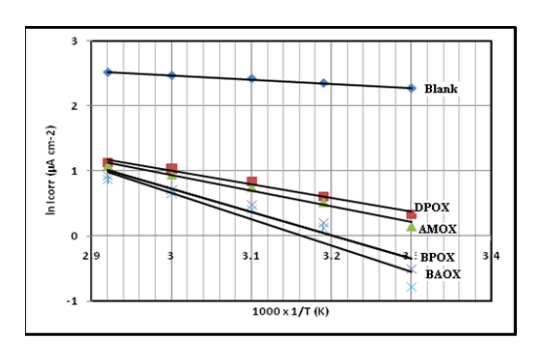
 $\textbf{Fig. 6} \ Tafel \ plots for copper-nickel \ alloy \ in \ natural \ sea \ water \ in \ the \ presence \ BAOX \ at \ different \ temperature$

The corrosion parameters and inhibition efficiencies are given in Table 4. The corrosion current density increases and the inhibition efficiency decreases with the increase of temperature both in the absence and presence of inhibitors, thus both corrosion current density and inhibition efficiency of the studied inhibitors are temperature-dependent in natural seawater.

Arrhenius equation was used to calculate the activation energy of the corrosion process. Fig. 7 presents the Arrhenius plots of natural logarithm of corrosion current density, ln $I_{\rm corr}$ against 1/T in the absence and presence of DPOX, AMOX, BPOX and BAOX in natural seawater. The value of $E_{\rm a}$ obtained in natural seawater containing inhibitors decreases with increase of temperature. The calculated values of activation energy from the slope in the absence and presence of optimum concentration of DPOX, AMOX, BPOX and BAOX in natural sea water are 12.50 kJmol $^{-1}$, 40.12 kJmol $^{-1}$, 46.23 kJmol $^{-1}$, 68.19 kJmol $^{-1}$ and 77.77 kJmol $^{-1}$ respectively. The increase in activation energy can be attributed to an appreciable decrease in the

adsorption of the inhibitor on the surface of the alloy with increasing temperature. The increase in solution temperature slightly shifts $E_{\rm corr}$ values and enhances both cathodic and anodic current densities. The decrease in inhibition efficiency with increasing temperature may be due to the increase in desorption of inhibitors.

Inhibitor	Temp	E _{corr} /	Icorr	βα	β _c	CR	IE
	(K)	mVvs.SCE	/μA cm ⁻²	(mVdec-1)	(mVdec-1)	(mmpy)	(%)
Blank	303	187	6.23	69	-121	7.185	-
	313	169	8.67	58	-128	9.999	-
	323	158	9.98	52	-134	11.51	-
	333	151	12.35	39	-143	14.24	-
	343	138	13.85	33	-151	15.97	-
	303	268	0.96	132	-57	1.107	84.59
	313	261	1.72	129	-63	1.983	80.16
DPOX	323	252	2.23	121	-73	2.571	77.65
	333	244	2.59	118	-78	2.987	79.02
	343	231	3.26	112	-82	3.759	76.47
	303	262	0.72	138	-52	0.830	88.44
AMOX	313	249	1.67	133	-55	1.926	80.74
	323	242	2.17	127	-60	2.503	78.25
	333	227	2.46	122	-68	2.837	80.08
	343	216	3.12	114	-76	3.598	77.49
	303	255	0.56	145	-50	0.646	91.01
BPOX	313	244	1.34	141	-53	1.545	84.54
	323	232	1.75	133	-59	2.018	82.46
	333	224	2.13	129	64	2.456	82.75
	343	216	2.89	117	-73	3.333	79.13
	303	236	0.31	148	-43	0.357	95.02
BAOX	313	217	1.13	143	-48	1.303	86.97
	323	204	1.56	137	-55	1.799	84.37
	333	183	1.97	130	-61	2.272	84.05
	343	177	2.49	123	-69	2.871	82.02



 $\textbf{Fig. 7} \ \, \textbf{Arrhenius plots for the brass in natural sea water containing optimum concentration of DPOX, AMOX, BPOX and BAOX}$

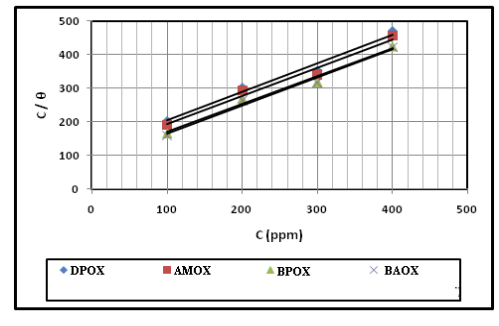


Fig. 8 Langmuir adsorption isotherm plot for the copper-nickel alloy in natural sea water containing different concentration of DPOX, AMOX, BPOX and BAOX

3.3 Adsorption Isotherm and Thermodynamic Parameters

The degree of surface coverage (θ) estimated at different concentrations of studied oxadiazole derivatives were tested graphically as to whether they fitted the Langmuir, shows a straight line indicating that adsorption follows the Langmuir adsorption isotherm as shown in Fig. 8. The high value of the adsorption equilibrium constant reflects the high adsorption ability of this inhibitor on alloy surface [19].

An increase in both K_{ads} and ΔG_{ads} values at $10^{\text{-}3}$ M concentration of DPOX, AMOX, BPOX and BAOX which support better adsorption of the inhibitor molecules on the metal surface. The negative value of ΔG_{ads} indicates spontaneous adsorption of the DPOX, AMOX, BPOX and BAOX on the copper-nickel alloy surface and also the strong interaction between inhibitor molecules and the metal surface. The values of ΔG_{ads} in the present study was more than -20 kJmol $^{\text{-}1}$, suggested that DPOX, AMOX, BPOX and BAOX at $10^{\text{-}2}\text{are}$ chemisorbed on the alloy surface.

It may be assumed that adsorption occurs due to the strong adsorption of water molecules on the surface of the alloy. It can be seen from the table that $K_{\rm ads}$ decreased with increase in temperature which indicates a decrease in the extent of adsorption of inhibitor molecules on the surface of the alloy. Fig. 9 shows the relation between ln $K_{\rm ads}$ and 1/T for DPOX, AMOX, BPOX and BAOX respectively and the thermodynamic parameters obtained are given in Table 5.

It is known that the ΔG values of DPOX, AMOX, BPOX and BAOX indicate the chemisorption mode. As the temperature increases, the value of free energy of adsorption decreases negatively indicating desorption of the studied inhibitors. The ΔH of inhibitors at 10^{-3} M indicates that the adsorption is an exothermic process. In the present case, the absolute values of enthalpy of the studied inhibitors are higher than 40 kJ mol⁻¹ confirming chemisorptions. It is observed that the ΔS values of DPOX, AMOX, BPOX and BAOX indicate chemisorptions mode. The negative values of ΔS in the present study are expected as the adsorption process is accompanied by a decrease in the disorder of the system due to the adsorption of the free oxadiazole derivatives onto the alloy surface [20].

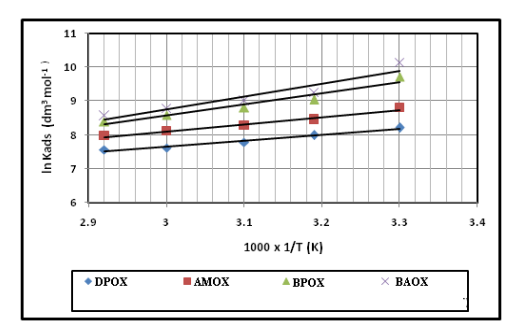


Fig. 9 Adsorption isotherm plot for DPOX, AMOX, BPOX and BAOX in natural sea water

Table 5 Thermodynamic parameters for the adsorption of oxadiazole derivatives on the alloy surface in natural sea water at different temperatures

Inhibitors	Temp (K)	K _{ads} dm ³ mol ⁻¹	-∆Gads	-∆H _{ads}	-ΔS
			(KJ mol-1)	(KJ mol-1)	(J mol ⁻¹ K ⁻¹)
	303	3661	31.18	45.21	46.30
	313	2937	31.06	45.21	45.20
HPBT	323	2394	31.68	45.21	41.88
	333	2012	32.18	45.21	39.12
	343	1913	33.01	45.21	35.56
	303	6667	37.06	47.85	35.61
BPBT	313	4731	32.16	47.85	50.12
	323	3919	33.01	47.85	45.94
	333	3319	33.57	47.85	42.88
	343	2934	34.22	47.85	39.73
	303	16494	33.16	58.39	83.26
OPBT	313	8440	32.29	58.39	83.38
	323	6623	34.41	58.39	74.24
	333	5378	34.90	58.39	70.54
	343	4389	35.37	58.39	67.11
	303	24997	35.64	61.43	85.11
OMBT	313	10351	34.12	61.43	96.83
	323	8219	34.99	61.43	81.85
	333	6466	35.41	61.43	78.13
	343	5269	35.89	61.43	74.46

3.4 Electrochemical Impedance Spectroscopy (EIS)

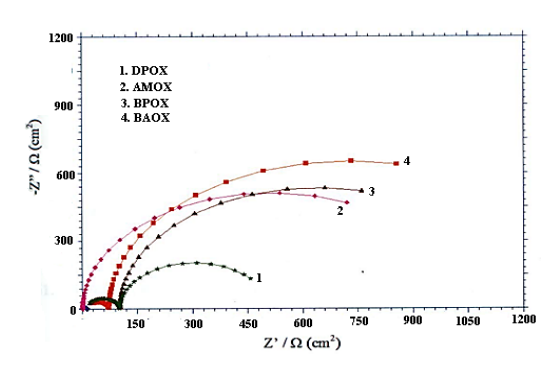
The corrosion behaviour of copper-nickel alloy in sea water in the presence of oxadiazole derivatives was investigated by EIS method at room temperature. The impedance diagrams were not perfect semicircles, which may be attributed to the frequency dispersion [21]. Nyquist plots of alloy in inhibited and uninhibited sea water containing optimum concentrations of DPOX, AMOX, BPOX and BAOX after immersion of 1 hr is

shown in Fig. 10. The percent inhibition efficiency (IE %) of corrosion alloy was calculated as follows [22]

IE % =
$$\frac{(R_{ct})^{-1} - (R_{ct(inh)})^{-1}}{(R_{ct})^{-1}} \times 100$$

where, R_{ct inh} and R_{ct} are the charge-transfer resistance values with and without inhibitors respectively. IE% attained 96.11 after immersion of 1hr with optimum concentration of BAOX, which was comparatively higher than that of DPOX, AMOX, and BPOX in natural sea water. This behaviour was attributed to more surface coverage of BAOX on the alloy surface from natural sea water. The inhibition efficiency values determined using the polarization curves were lower than those determined by EIS experiments, this difference was probably due to shorter immersion time in the case of the polarization measurements. Impedance parameters derived from these investigations are given in Table 6. In the presence of optimum concentration of inhibitors, Rct values increased, whereas Cdl values tended to decrease. The decrease in C_{dl} values was caused by adsorption of oxadiazole derivatives on the alloy surface. The tendency to decrease in C_{dl}, which can result from a decrease in local dielectric constant and/or an increase in the thickness of the electrical double layer, suggests that the oxadiazole derivatives function by adsorption at the metalsolution interface [23]. The change in R_{ct} and C_{dl} values was caused by the gradual replacement of water molecules by the chloride ions and adsorption of the organic molecules on the metal surface, reducing the extent of dissolution.

The molecular structure normally determines the type of adsorption on alloy surface [24]. Oxadiazole derivatives viz., DPOX, AMOX, BPOX and BAOX show differences in their inhibition efficiency due to the difference in their molecular structures. Of the oxadiazole derivatives studied, BAOX has the highest inhibition efficiency and this corresponds well with the polarization measurements. The % IE calculated from EIS shows the same trend as those estimated from polarisation measurements i.e., polarization measurements and EIS study complement each other well.



 $\textbf{Fig. 10} \ \ \text{Nyquist diagram of cupro-nickel alloy in natural sea water containing optimum concentration of oxadiazole derivatives after 1 hr immersion$

Table 6 Impedance parameters of copper-nickel alloy in natural sea water containing optimum concentration of oxadiazole derivatives

Inhibitor	R _{ct} x 10 ⁴ /ohm cm ²	C _{dl/} μFcm ⁻²	Inhibition Efficiency/%
Blank	0.96	33.34	-
DPOX	14.84	0.143	93.34
AMOX	19.96	0.13	95.19
BPOX	20.87	0.102	95.40
BAOX	24.68	0.089	96.11

3.5 Solution Analysis by ICP-AES

The results of solution analysis in the absence and presence of DPOX, AMOX, BPOX and BAOX at their optimum concentration level in natural sea water are given in Table 6. It can be observed that both copper and nickel were present in the solution whereas in the presence of inhibitors, which are able to minimize the dissolution of both copper and nickel. The data recorded in table illustrate that the percent inhibition efficiency against the dissolution of nickel was correspondingly high as compared to the dissolution of copper. This indicates the excellent inhibition efficiency of inhibitors to prevent the dissolution of alloy in natural sea water. Among the inhibitors studied, BAOX shows highest inhibition efficiency in the dissolution of alloy in sea water. The percent inhibition efficiency against the dissolution of Ni was correspondingly high i.e. 94.50% can be achieved in the presence of BAOX containing natural sea water, indicating that the preferential dissolution of nickel was almost completely minimized.

Table 7 Effect of optimum concentrations of DPOX, AMOX, BPOX and BAOX on the dissolution of copper-nickel alloy natural sea water

	Solution analy	/sis	Percent i	nhibition	
Inhibitors	Cu	Ni	Cu/	Ni/	
	x 10-6 / M	x 10-6//M	%	%	
Blank	0.946	12.36	-	-	
DPOX	0.132	1.18	86.05	90.45	
AMOX	0.102	0.98	89.22	92.07	
BPOX	0.089	0.82	90.59	93.37	
BAOX	0.076	0.68	91.97	94.50	

4. Conclusion

Oxadiazole derivatives DPOX, AMOX, BPOX and BAOX show good inhibition efficiency in natural sea water. BAOX exhibits highest inhibition efficiency. The polarization data indicate that the corrosion rate increases and inhibition efficiency decreases with increase of temperature. The inhibitors easily adsorb on the alloy surface at the corrosion potential and form a protective complex with the Cu (I) ion, controlling copper-nickel alloy from corrosion. Electrochemical impedance spectroscopy shows that $R_{\rm ct}$ values increase, while $C_{\rm dl}$ values decrease in the presence of oxadiazole derivatives. The low $C_{\rm dl}$ value obtained in the presence of inhibitors indicate the formation of thicker inhibitor film on the metal surface. Solution analysis reveals that the oxadiazole derivatives excellently prevent the dissolution of copper and nickel.

References

- P.T. Gilbert, Metal/environment reactions, In Corrosion: Metal/environment Reactions (Ed: L.L. Shreir), Newness-Butterworths, London, 1976.
- [2] R. Gasparac, C.R. Martin, E. Stupnisek-Lisac, Z. Mandic, In situ studies of imidazole and its derivatives as copper corrosion inhibitors, J. Electrochem. Soc. 147 (2000) 548-551.
- [3] A. Nagiub, F. Mansfeld, Evaluation of corrosion inhibition of brass in chloride media using EIS and ENA, Corros. Sci. 43 (2001) 2147-2171.
- [4] C.A. Powell, Marine applications of copper-nickel alloys, section 1: copper-nickel alloys-resistance to corrosion and biofouling, Technical Reports, Copper Development Association, Potters Bar, United Kingdom, 1998.
- [5] F. Mansfeld, B.J. Little, Microbiologically influenced corrosion of copper based materials exposed to natural seawater, Electrochim. Acta. 37 (1992) 2291-2297.
- [6] A. Hall, A.J.M. Baker, Settlement and growth of copper tolerant *Ectocarpus siliculosus* (Dillw.) Lyngbye on different copper-based antifouling surfaces under laboratory conditions, Mater. Sci. 20 (1985) 1111-1118.

- [7] C. Kato, B.G. Ateya, J.E. Castle, H.W. Pickering, On the mechanism of corrosion of Cu-9.4Ni-1.7Fe alloy in air saturated aqueous NaCl solution-I, Kinetic investigations, J. Electrochem. Soc. 127 (1980) 1890-1896.
- [8] S. Cere, M. Vazquez, Properties of the passive films present on copper and copper-nickel alloys in slightly alkaline solutions, J. Mater. Sci. Lett. 21 (2002) 493-495
- [9] J.O.M. Bockris, B.T. Rubin, A. Despic, B. Lovrecek, The electro dissolution of copper nickel alloys, Electrochim. Acta. 17 (1972) 973-999.
- [10] R.F. North, M.J. Pryor, The influence of corrosion product structure on the corrosion rate of Cu-Ni alloys, Corros. Sci. 10 (1970) 297-311.
- [11] Y.M. Kolotyrkin, The electrochemistry of alloys, Electrochim. Acta. 25 (1980) 89-96.
- [12] R. Walker, Aqueous corrosion of Tin-Bronze and inhibition by benzotriazole, Corros. 56 (2000) 1211-1219.
- [13] Brusic, M.A. Frisch, B.N. Eldridge, P. Novac, F. Bkaufman, B.M. Rusch, et al., Study of the benzotriazole efficiency as a corrosion inhibitor for copper in humid air plasma, J. Electrochem. Soc. 138 (1991) 2253-2264.
- [14] W.A. Badawy, K.M. Ismail, A.M. Fathi, Corrosion control of Cu-Ni alloys in neutral chloride solutions by amino acids, Electrochim. Acta. 59 (2006) 4182-4189.
- [15] M. Benmessaoud, K. Es-salah, N. Hajjaji, H. Takenouti, A. Srhiri, M. Ebentouhami, Inhibiting effect of 2-mercaptobenzimidazole on the corrosion of Cu-30Ni alloy in aerated 3% NaCl in presence of ammonia, Corros. Sci. 49 (2007) 3880-3888.
- [16] N.K. Allam, E.A. Ashour, H.S. Hegazy, B.E. El-Anadouli, B.G. Ateya, Effects of benzotriazole on the corrosion of Cu-Ni alloy in sulphide-polluted salt water, Corros. Sci. 47 (2005) 2280-2292.
- [17] M.A. Quraishi, R. Sardar, Dithiazolidines-A new class of heterocyclic inhibitors for prevention of mild steel corrosion in hydrochloric acid solution, Corros. 58 (2002) 103-107
- [18] M.G. Fontana, Corrosion Engineering, McGraw Hill Book Company, Singapore, 1987.
- [19] J. Morales, G.T. Fernandez, P. Esparza, S. Gonzalez, R.C. Salvarezza, et al., A comparative study on the passivation and localized corrosion of brass in borate buffer solutions containing sodium chloride-I Electrochemical data, Corros. Sci. 37 (1995) 211-229.
- [20] M.G. Biton, D. Aurbach, P. Mishkov, D. Ilzycer, On the electrochemical behavior and passivation of copper and brass (Cu70/Zn30) electrodes in concentrated aqueous KOH solutions, J. Electrochem. Soc. 153 (2006) 555-563.
- [21] F. Mansfeld, M.W. Kending, S. Tsai, Determination of corrosion rates by electrochemical DC and AC methods, Corros. Sci. 21 (1981) 647-672.
- [22] S.S.A. El-Rehim, M.A.M. Ibrahim, 4-Aminoantipyrine as an inhibitor of mild steel corrosion in HCl solution, J. Appl. Electrochem. 29 (1999) 593-599.
- [23] M.M. Singh, R.B. Rastogi, B.N. Upadhyay, Thiosemicarbazide, phenyl isothiocyanate and their condensation product as corrosion inhibitors of copper in aqueous chloride solutions, Mater. Chem. Phy. 80 (2003) 283-293.
- [24] J.P. Ferreira, J.A. Rodrigues, I.T.E. Fonseca, Copper corrosion in buffered and non-buffered synthetic seawater: a comparative study, J. Solid State Electrochem. 8 (2004) 260-271.